Supplementary Figures and Tables

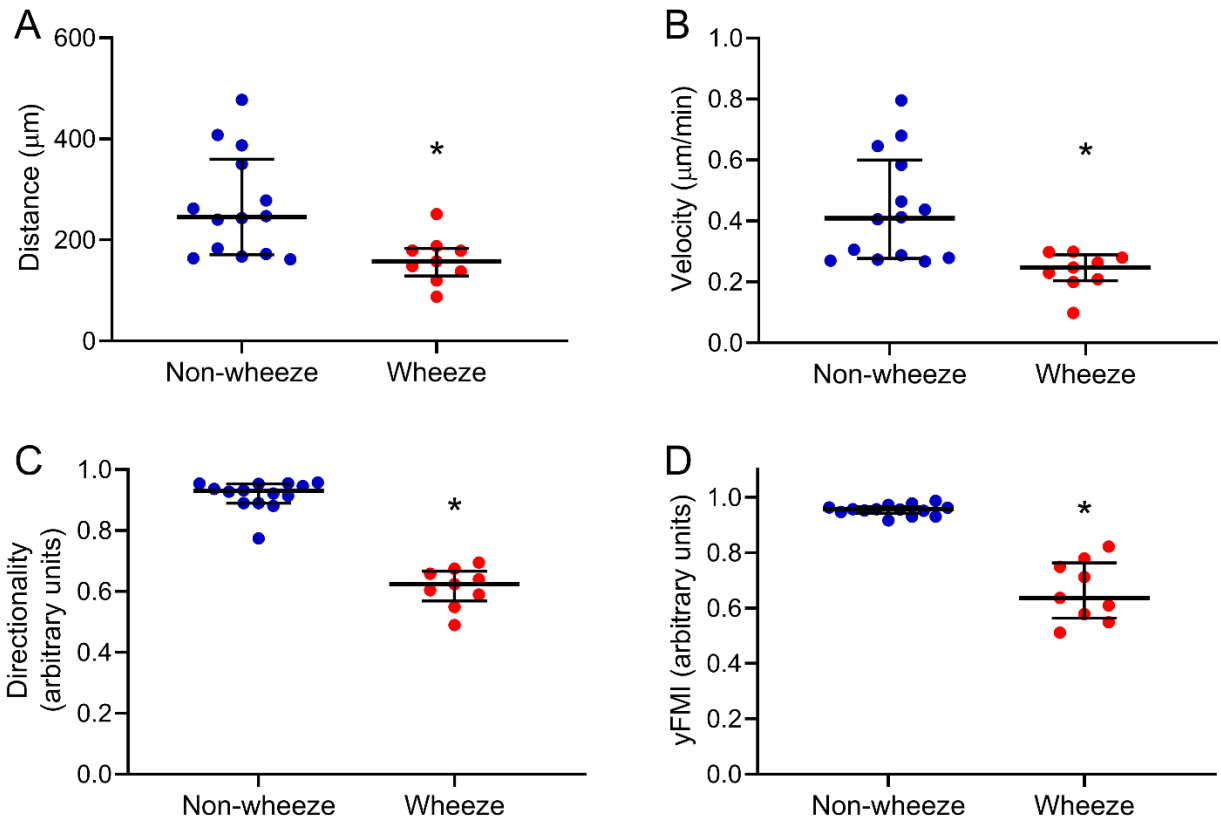

Figure S1. Cell migration trajectories for each patient.

All leading edge pAEC migration trajectories were represented as an average for each child with and without wheeze (complete data presented in Figure 1). Despite the heterogeneous response to wounding observed at the individual leading edge cell level, the patient-specific pAEC repair response was characterized by defective cell migration. Specifically, leading edge cells of children with wheeze migrated shorter average distances (A) and at slower velocity (B) than their non-wheezing counterparts ($p<0.050$). Furthermore, leading edge pAEC of children with wheeze demonstrated migration trajectories with significantly less directionality (C) and yFMI (D), indicating a uniform loss of coordination in their response to wounding. Cell migration trajectory data were generated from leading edge cell tracks of children with wheeze (n=14) and without wheeze (n=9) respectively. Data were represented as median ± IQR, *$p<0.050$, Mann-Whitney U-test.

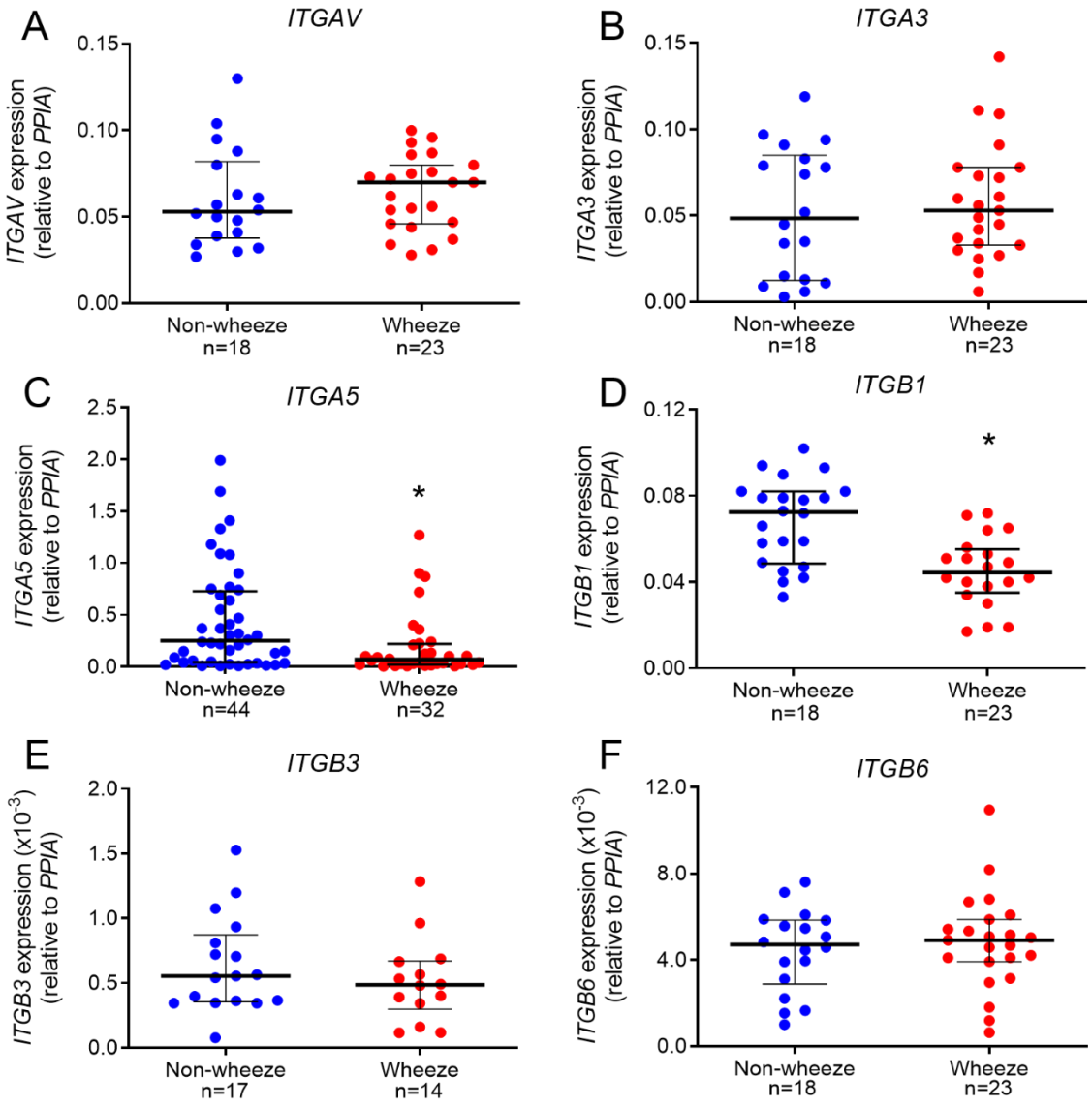
A
ITGAV
ITGAV expression (relative to PPIA)
0.15
0.10
0.05
0.00
Non-wheeze n=18
Wheeze n=23
B
ITGA3
ITGA3 expression (relative to PPIA)
0.15
0.10
0.05
0.00
Non-wheeze n=18
Wheeze n=23
C
ITGA5
ITGA5 expression (relative to PPIA)
2.5
2.0
1.5
1.0
0.5
0.0
*
Non-wheeze n=44
Wheeze n=32
D
ITGB1
ITGB1 expression (relative to PPIA)
0.12
0.08
0.04
0.00
*
Non-wheeze n=18
Wheeze n=23
E
ITGB3
ITGB3 expression (x10-3) (relative to PPIA)
2.0
1.5
1.0
0.5
0.0
Non-wheeze n=17
Wheeze n=14
F
ITGB6
ITGB6 expression (x10-3) (relative to PPIA)
12.0
8.0
4.0
0.0
Non-wheeze n=18
Wheeze n=23

Figure S2. Profiling the expression of fibronectin-binding integrin subunits in pediatric airway epithelium.

mRNA expression of integrin α (A,B,C) and β (D,E,F) subunits were measured in *ex vivo* pAEC of children with and without wheeze. No significant differences were observed between pAEC from children with and without wheeze in mRNA expression of *ITGAV* (A), *ITGA3* (B), *ITGB3* (E) and *ITGB6* (F) ($p>0.050$). In contrast, pAEC from children with wheeze displayed significantly lower mRNA levels of both *ITGA5* (C; $*p<0.050$) and β1 (D; $*p<0.050$) compared to their non-wheezing counterparts. Each dot represents the mean of two technical replicates from a single patient sample. Data were represented as median ± IQR and tatistical differences between groups ($*p<0.050$) were determined using the Mann-Whitney U-test. Sample sizes in each patient cohort are indicated under each integrin subunit panel.

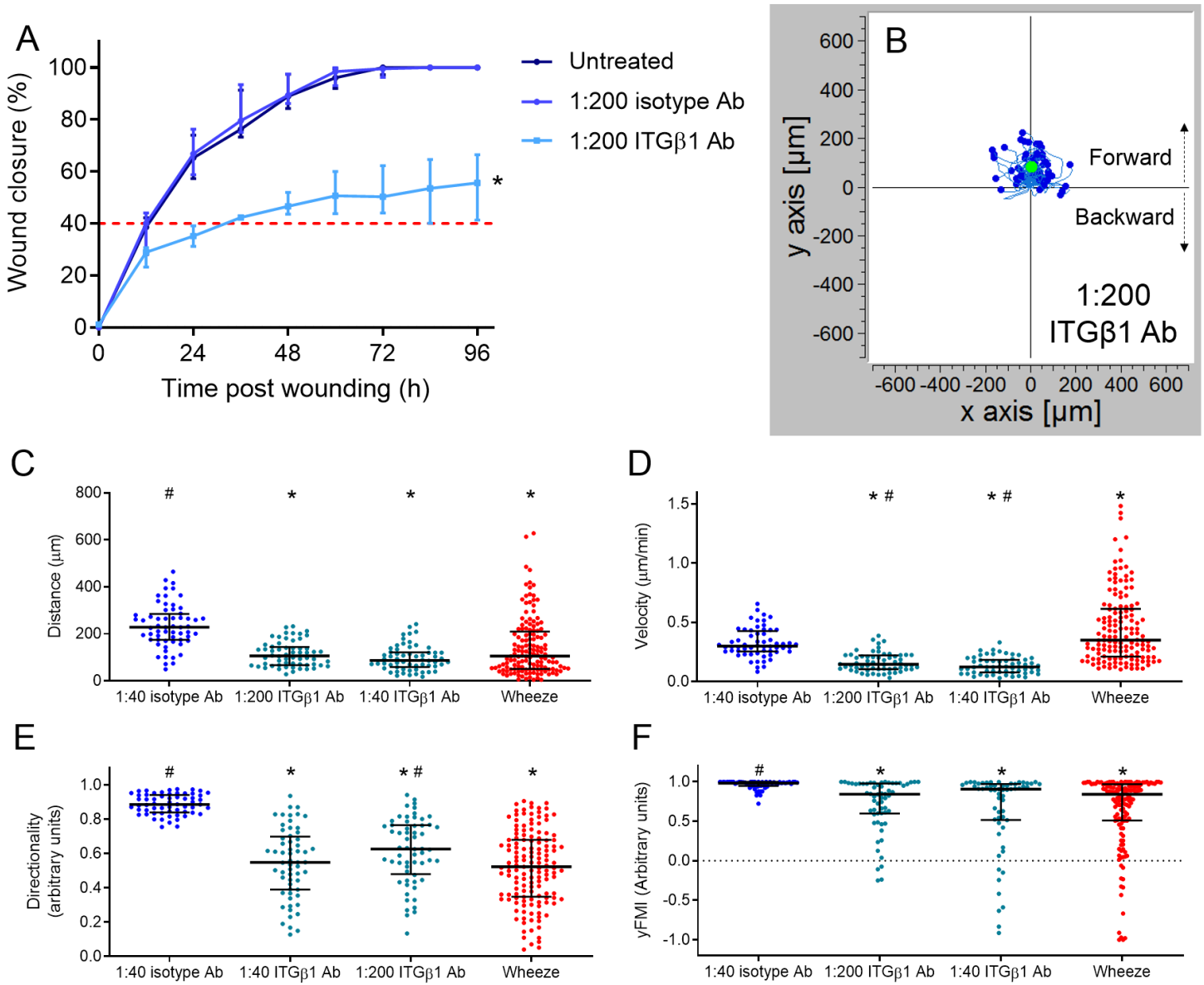
A
Wound closure (%)
Time post wounding (h)
Untreated
1:200 isotype Ab
1:200 ITGβ1 Ab
B
y axis [µm]
x axis [µm]
Forward
Backward
1:200
ITGβ1 Ab
C
Distance (µm)
D
Velocity (µm/min)
E
Directionality
(arbitrary units)
F
yFMI (Arbitrary units)
1:40 isotype Ab
1:200 ITGβ1 Ab
1:40 ITGβ1 Ab
Wheeze

Figure S3. Functional blocking of integrin β1 in pAEC from children without wheeze. (A) Blocking β1 integrin function (1:200 dilution; IgG1κ, P5D2) significantly reduced wound closure rates in pAEC from non-wheezing children to similar ranges as those observed in wheezers (red dashed line). Matching dilution of isotype control antibody (IgG1κ, MOPC-21) or untreated pAEC reached full wound closure by 72h post wounding. Data were represented as median ± IQR. *Statistical significance relative to the non-wheeze cohort ($p<0.050$; Mann-Whitney U-test). (B) Cultures treated with 1:200 dilution of anti-β1 integrin antibody in culture media migrated less far into the wound, lacking cell directionality and specificity towards the wound center. Individual cell tracks (n=60 tracks from cultures of 4 children without wheeze) were transposed so that each track had its start at the origin. Although treatment of pAEC from non-wheezing children with 1:40 dilution of isotype control antibody had no effect on cell migration (C-F), treatment with either 1:40 or 1:200 dilutions of anti-β1 integrin antibody abrogated cell migration (C-F) by blocking distance migrated (C), velocity (D), directionality (E) and centrality (yFMI, F). All experiments were completed with pAEC cultures from 4 children without wheeze and data were represented as median ± IQR. Statistical differences between treatment and isotype control (*$p<0.050$), or wheeze group ($^{\#}p<0.050$) were determined using the Kruskal-Wallis ANOVA with Dunn's post-test for multiple comparisons. The wound closure data for the untreated group were also presented in Figure 2.

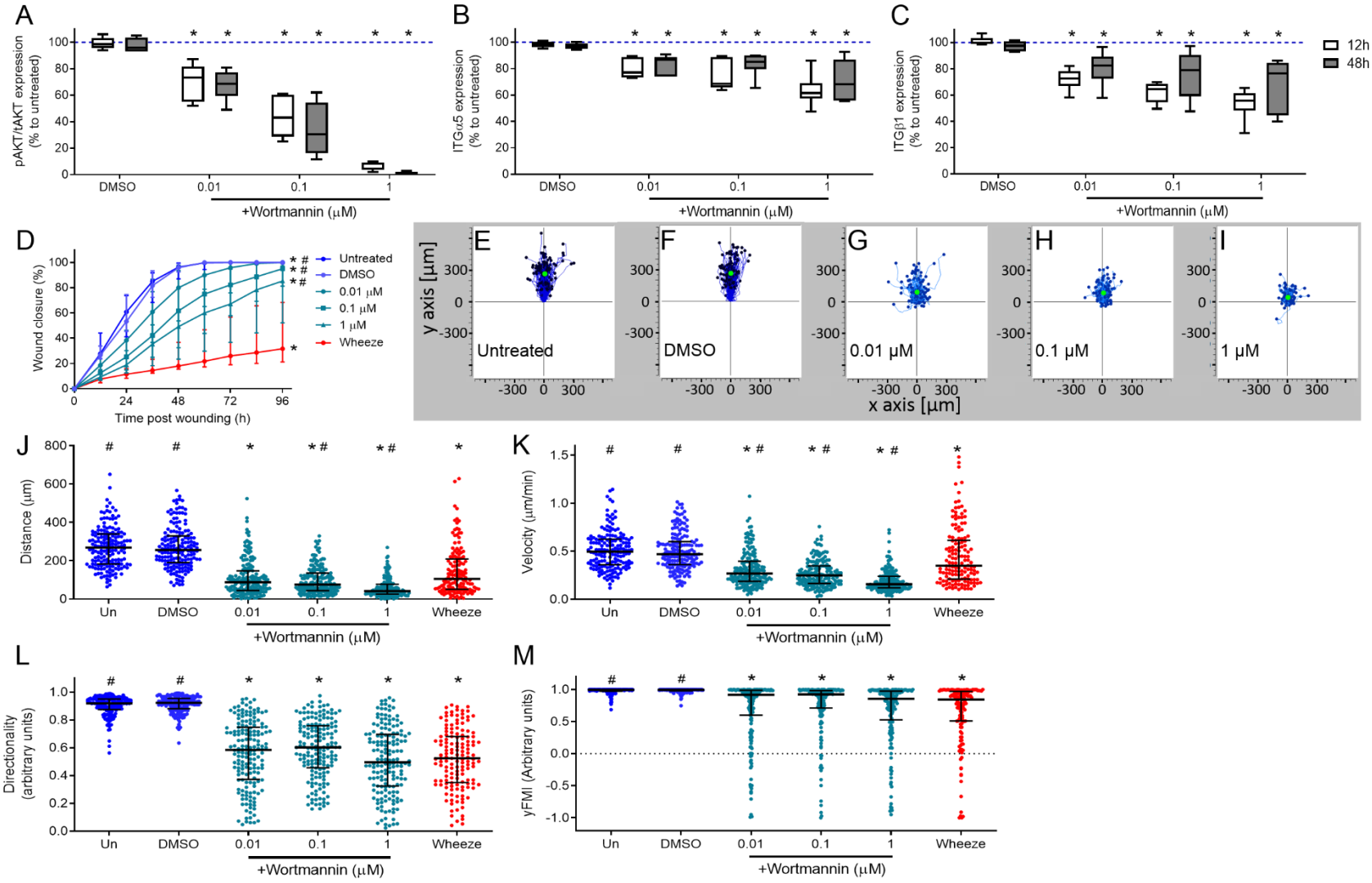
A
pAKT/tAKT expression (% to untreated)
DMSO
0.01
0.1
1
+Wortmannin (μM)
B
ITGα5 expression (% to untreated)
C
ITGβ1 expression (% to untreated)
12h
48h
D
Wound closure (%)
Time post wounding (h)
Untreated
DMSO
0.01 μM
0.1 μM
1 μM
Wheeze
E
F
G
H
I
y axis [μm]
x axis [μm]
J
Distance (μm)
Un
K
Velocity (μm/min)
L
Directionality (arbitrary units)
M
yFMI (Arbitrary units)

Figure S4. Dampened PI3K/Akt signaling attenuates airway epithelial repair and reduces integrin α5β1 expression.

pAEC from children without wheeze were treated with different concentrations (0.01, 0.1, 1 μM) of the pan-PI3K inhibitor, Wortmannin. (A) Wortmannin inhibited activation of PI3K and phosphorylation of its downstream effector, Akt (serine residue 473), at 12h and 48h post treatment. Inhibition of PI3Ks in pAEC from children without wheeze resulted in significant reduction of integrin subunits α5 (B) and β1 (C) cell membrane expression in a concentration-dependent manner at 12h and 48h post Wortmannin treatment. (D) Treatment of pAEC cultures from non-wheezing children with Wortmannin at the time of scratch wounding resulted in a concentration-dependent reduction in closure rates, although 0.1 % (v/v) DMSO vehicle control was not significantly altered compared to untreated cultures. Although treatment of pAEC from non-wheezing children with 0.1% (v/v) DMSO vehicle control had no effect on cell migration (E-F), Wortmannin treatment attenuated cell migration in a concentration-dependent manner (G-I) by inhibiting distance migrated (J), velocity (K), directionality (L) and centrality (yFMI, M) of Wortmannin-treated cultures in a concentration-dependent manner. All experiments were completed with pAEC from 6 children without wheeze and data were represented as either box and whisker (min/max) or dot plots with median ± IQR. Statistical differences between treatment and untreated control (*$p<0.050$), or wheeze group ($^{\#}p<0.050$) were determined using the Kruskal-Wallis ANOVA with Dunn's post-test for multiple comparisons. The wound closure (D) and cell migration parameters (J-M) for the untreated wheeze and non-wheeze groups were also presented in Figure 4 and were utilized for baseline response purposes.

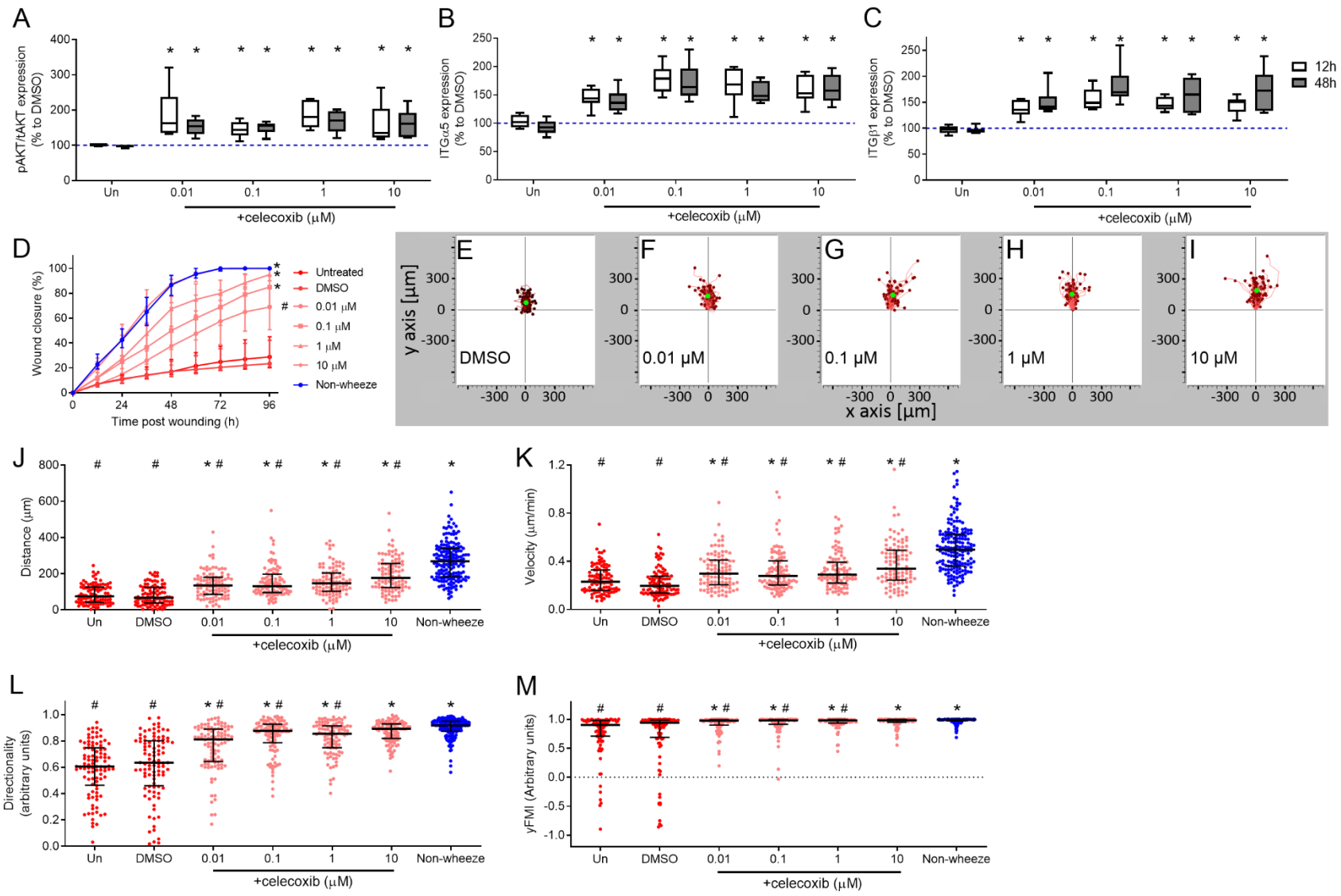
A
pAKT/tAKT expression (% to DMSO)
Un
0.01
0.1
1
10
+celecoxib (μM)
B
ITGα5 expression (% to DMSO)
C
ITGβ1 expression (% to DMSO)
12h
48h
D
Wound closure (%)
Time post wounding (h)
Untreated
DMSO
0.01 μM
0.1 μM
1 μM
10 μM
Non-wheeze
E
F
G
H
I
y axis [μm]
x axis [μm]
DMSO
0.01 μM
0.1 μM
1 μM
10 μM
J
Distance (μm)
DMSO
Non-wheeze
K
Velocity (μm/min)
L
Directionality (arbitrary units)
M
yFMI (Arbitrary units)

Figure S5. Repair of pAEC from children with wheeze can be modulated by COX2 inhibitor, celecoxib, treatment via the PI3K/Akt/integrin α5β1 axis.

pAEC from children with wheeze were treated with different concentrations (0.01, 0.1, 1, 10 μM) of COX2 inhibitor, celecoxib. (A) Celecoxib treatment resulted in phosphorylation of Akt (serine residue 473), at 12h and 48h post treatment. Significant activation of integrin subunits α5 (B) and β1 (C) cell membrane expression was observed in treated cultures from children with wheeze at both 12h and 48h. (D) Treatment of pAEC cultures from wheezing children with celecoxib at the time of scratch wounding resulted in increase in closure rates in a concentration-dependent manner to similar levels as their non-wheezing counterparts. Although treatment of pAEC from wheezers with 0.13% (v/v) DMSO vehicle control had no effect on cell migration (E), celecoxib treatment enhanced cell migration in a concentration-dependent manner (F-I) by stimulating distance migrated (J), velocity (K), directionality (L) and centrality (yFMI, M). All experiments were completed with pAEC cultures from 6 children with wheeze and data were represented as either box and whisker (min/max) or dot plots with median ± IQR. Statistical differences between treatment and untreated control (*$p<0.050$), or non-wheeze group ($^{\#}p<0.050$) were determined using the Kruskal-Wallis ANOVA with Dunn's post-test for multiple comparisons. The wound closure (D) and cell migration parameters (J-M) for the untreated non-wheeze group were also presented in Figure 4, as well as the untreated, DMSO and 10 μM celecoxib groups in Figure 6.

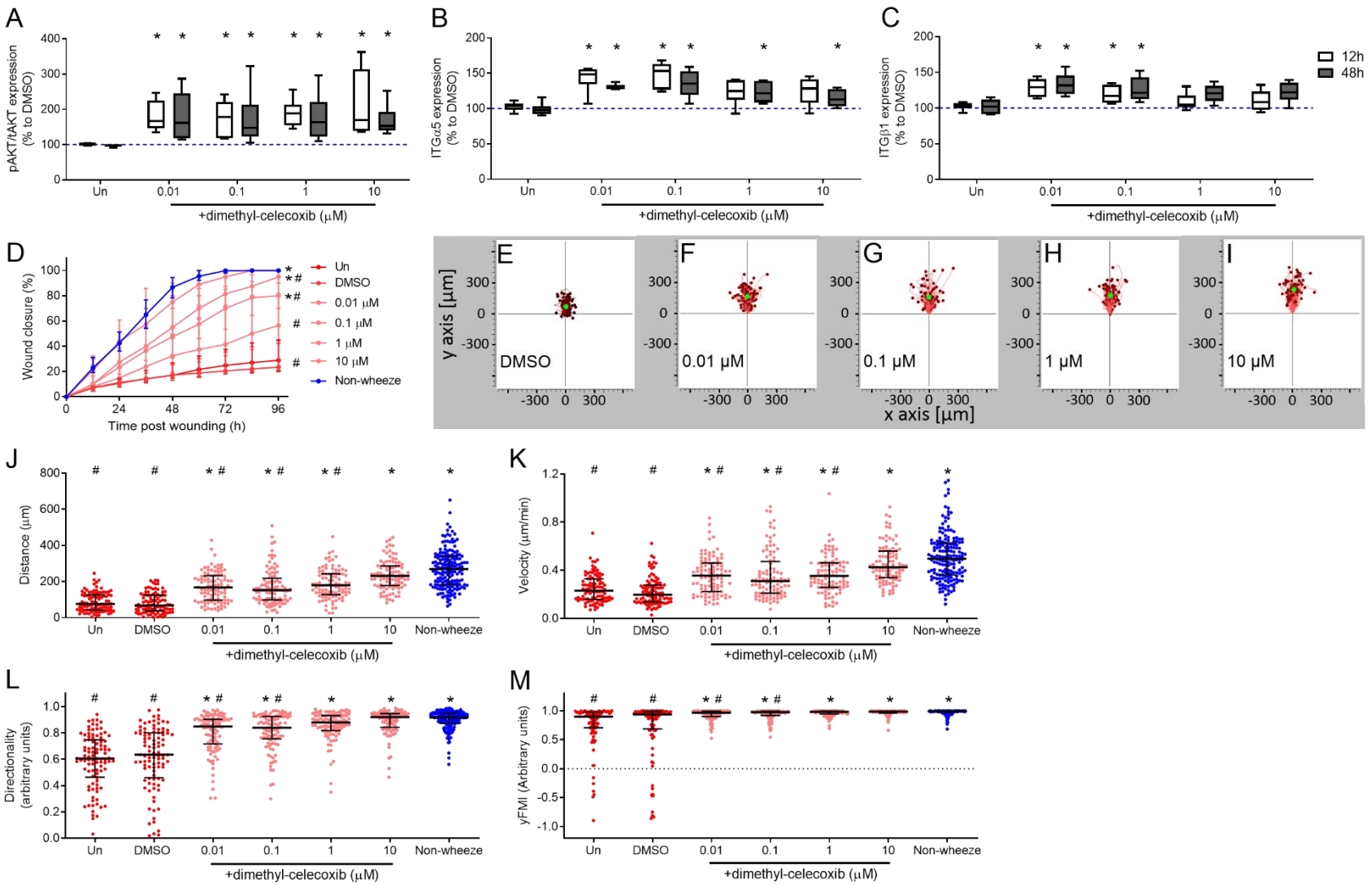
A
pAKT/tAKT expression (% to DMSO)
+dimethyl-celecoxib (μM)
B
ITGα5 expression (% to DMSO)
C
ITGβ1 expression (% to DMSO)
12h
48h
D
Wound closure (%)
Time post wounding (h)
Un
DMSO
0.01 μM
0.1 μM
1 μM
10 μM
Non-wheeze
E
F
G
H
I
y axis [μm]
x axis [μm]
J
Distance (μm)
K
Velocity (μm/min)
L
Directionality (arbitrary units)
M
yFMI (Arbitrary units)

Figure S6. Repair of pAEC from children with wheeze can be modulated by dimethyl-celecoxib, in a COX2-independent manner, via the PI3K/Akt/integrin α5β1 axis.

pAEC from children with wheeze were treated with different concentrations (0.01, 0.1, 1, 10 μM) of dimethyl-celecoxib, a celecoxib analogue lacking COX2 inhibitory activity. (A) Dimethyl-celecoxib treatment resulted in phosphorylation of Akt (serine residue 473), at 12h and 48h post treatment. Significant activation of integrin subunits α5 (B) and β1 (C) cell membrane expression was observed in treated cultures from children with wheeze. (D) Treatment of pAEC cultures from wheezers with dimethyl-celecoxib at the time of scratch wounding resulted in increase in wound closure rates where complete repair was observed with 10 μM dimethyl-celecoxib treatment. Although treatment of pAEC from wheezers with 0.13% (v/v) DMSO vehicle control had no effect on cell migration (E), dimethyl-celecoxib treatment enhanced cell migration in a concentration-dependent manner (F-I) by stimulating distance migrated (J), velocity (K), directionality (L) and centrality (yFMI, M). All experiments were completed with pAEC cultures from 6 children with wheeze and data were represented as either box and whisker (min/max) or dot plots with median ± IQR. Statistical differences between treatment and untreated control (*$p<0.050$), or non-wheeze group ($^{\#}p<0.050$) were determined using the Kruskal-Wallis ANOVA with Dunn's post-test for multiple comparisons. The wound closure (D) and cell migration parameters (J-M) for the untreated non-wheeze group were also presented in Figure 4, as well as the untreated, DMSO and 10 μM dimethyl-celecoxib groups in Figure 6.

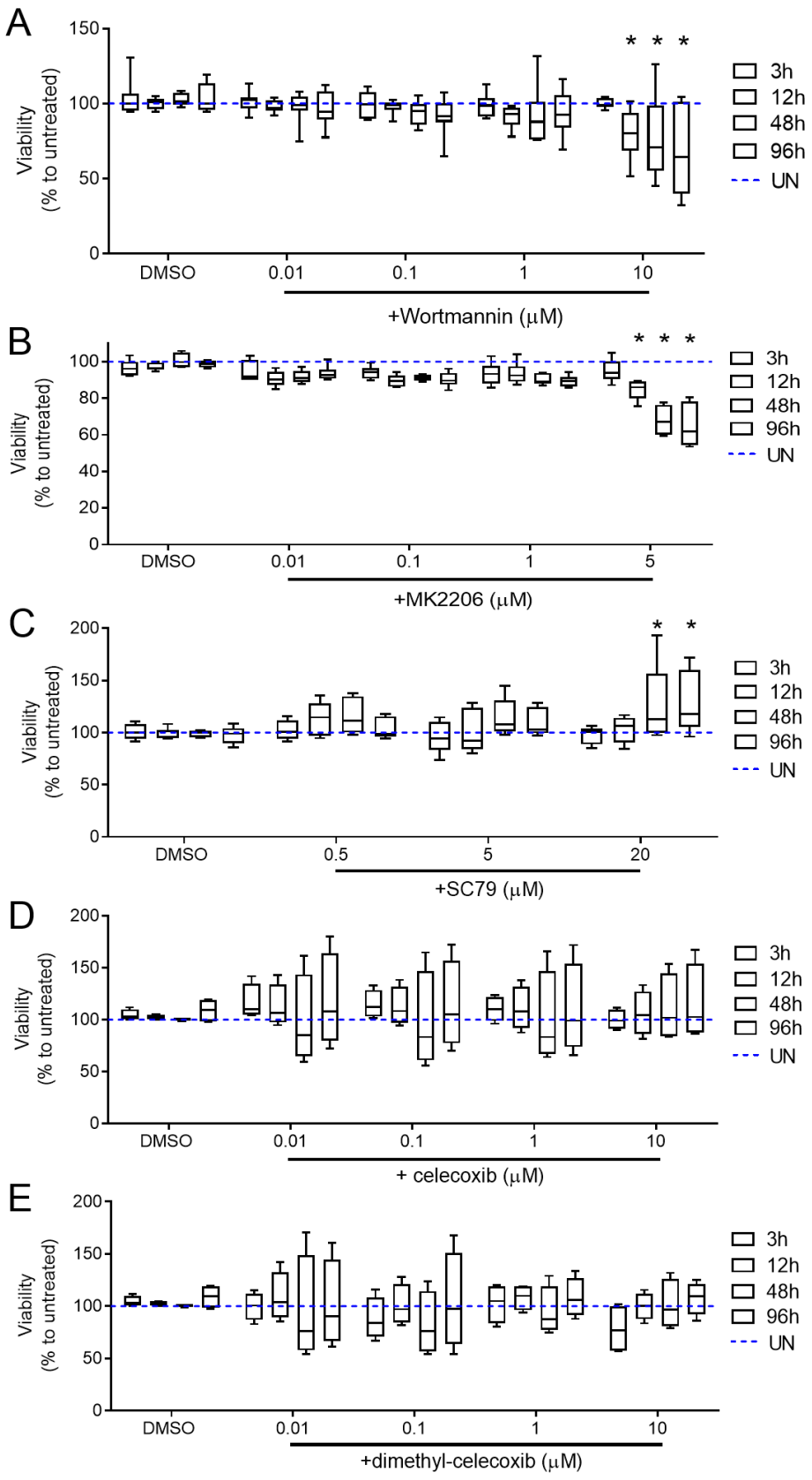
A
Viability (% to untreated)
150
100
50
0
DMSO
0.01
0.1
1
10
+Wortmannin (μM)
* * *
3h
12h
48h
96h
UN
B
Viability (% to untreated)
100
80
60
40
20
0
DMSO
0.01
0.1
1
5
+MK2206 (μM)
* * *
3h
12h
48h
96h
UN
C
Viability (% to untreated)
200
150
100
50
0
DMSO
0.5
5
20
+SC79 (μM)
* *
3h
12h
48h
96h
UN
D
Viability (% to untreated)
200
150
100
50
0
DMSO
0.01
0.1
1
10
+ celecoxib (μM)
3h
12h
48h
96h
UN
E
Viability (% to untreated)
200
150
100
50
0
DMSO
0.01
0.1
1
10
+dimethyl-celecoxib (μM)
3h
12h
48h
96h
UN

Figure S7. Cell viability of pAEC cultures treated with wortmannin, MK2206, SC79, celecoxib and dimethyl-celecoxib.

pAEC cultures from 6 children without wheeze were treated with different concentrations (0.01, 0.1, 1, 10 μM) of the pan-PI3K inhibitor, wortmannin (A) or specific Akt inhibitor, MK2206 (B; 0.01, 0.1, 1, 5 μM). (C) Cultures from 6 children with wheeze were treated with different concentrations (0.5, 5, 20 μM) of the Akt activator, SC79. (D-E) Cultures from 6 children with wheeze were treated with different concentrations (0.01, 0.1, 1, 10 μM) of celecoxib (D) or dimethyl-celecoxib (E). Data were represented as box and whisker (min/max) with median ± IQR and group differences were considered statistically significant if $p<0.050$ (Kruskal-Wallis ANOVA with Dunn's post-test for multiple comparisons). All experiments were completed in two technical replicates.

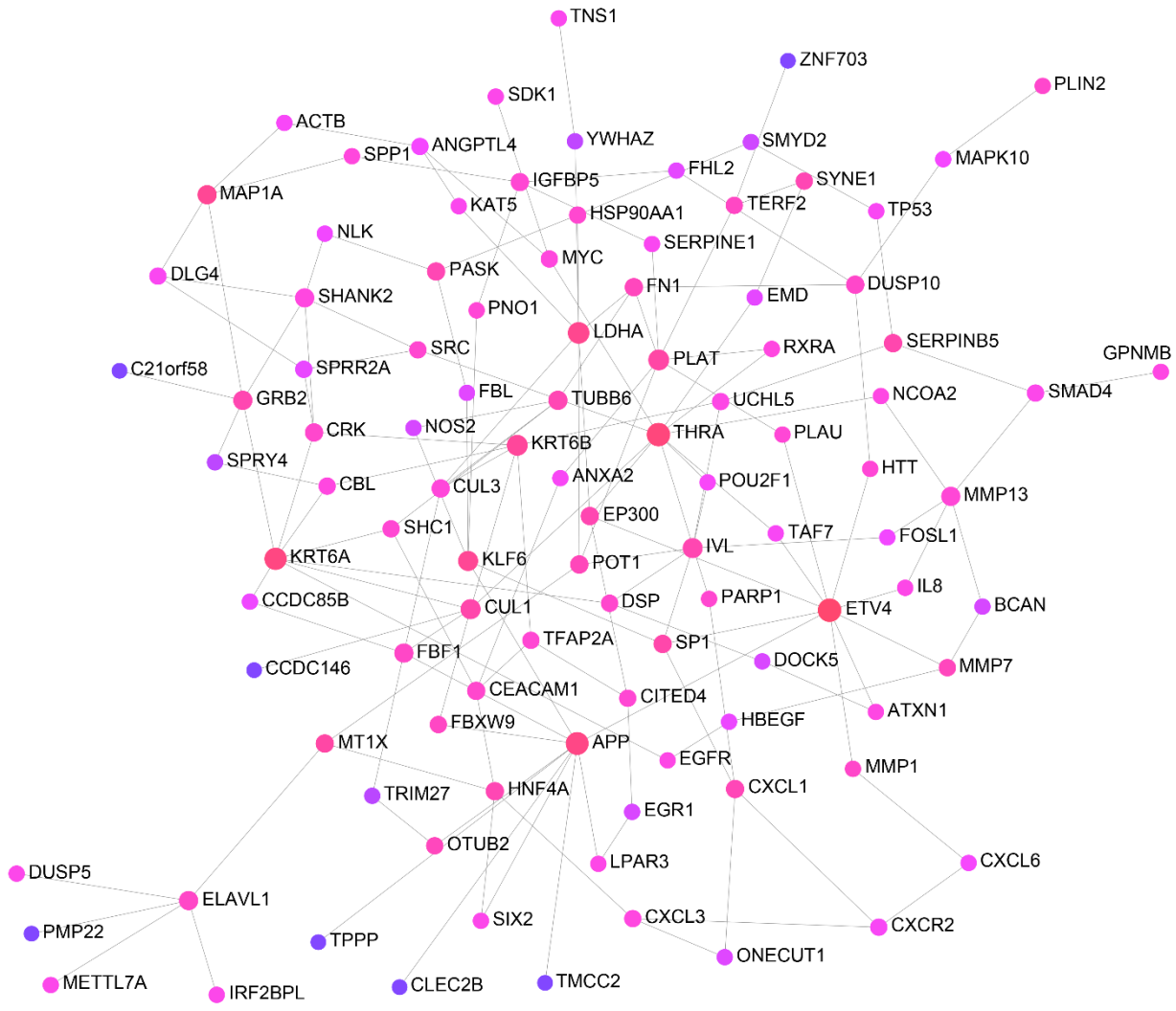

Figure S8. Network diagram of common differentially expressed genes between defective pAEC repair gene signature from children with wheeze and a published transcriptomic dataset of pAEC from adults with doctor-diagnosed asthma.

(A) Minimum network map of common differentially expressed genes between the defective pAEC repair discovery dataset and adult stable, mild asthma dataset. Genes are highlighted as highly interconnected (pink) or weakly interconnected (purple) according to known protein:protein interactions from published studies (prior knowledge). Larger nodes have more connections.

Table S1. Defective pAEC repair associates with wheeze in both pre-school and school-aged children.

	Number	Estimate	Standard Error	z value	Pr (> |z|)
Pre-school children (n=55)					
Defective pAEC repair	16	*N/A*	*N/A*	*N/A*	*N/A*
Wheeze	27	-2.705	0.834	-3.243	***1.184e-03 ****
Sex, M/F	31/24	-0.533	0.698	-0.764	4.448e-01
School-aged children (n=63)					
Defective pAEC repair	32	*N/A*	*N/A*	*N/A*	*N/A*
Wheeze	19	-2.398	0.778	-3.082	***2.060e-02 ****
Sex, M/F	43/21	-0.405	0.671	-0.603	5.467e-01

pAEC – primary airway epithelial cell; N/A – not applicable; M – male; F, female; *p<0.050.

Table S2. Defective pAEC repair associates with school-aged physician-diagnosed asthma.

School-aged children	**Non-asthma**	**Asthma**
Complete pAEC repair	31	0
Defective pAEC repair	10	22

pAEC – primary airway epithelial cell

Table S3. Upregulated genes in pAEC from children with wheeze at 24h post wounding compared to their non-wheezing counterparts.

Refer to MS Excel spreadsheet (supplementary).

Table S4. Downregulated genes in pAEC from children with wheeze at 24h post wounding compared to their non-wheezing counterparts.

Refer to MS Excel spreadsheet (supplementary).

Table S5. Canonical pathway analysis of differentially expressed genes in pAEC from children with wheeze at 24h post wounding compared to their non-wheezing counterparts.

Refer to MS Excel spreadsheet (supplementary).

Table S6. Upstream transcriptional regulators of integrin α5β1.

Refer to MS Excel spreadsheet (supplementary).

Table S7. Literature search for upstream regulators of both *ITGA5* and *ITGB1*, and selected keywords using PubMatrix.

Upstream Regulator	cell migration	repair	asthma	airway	airway epithelial cell
Akt	11033	3241	319	411	187
PI3K	5542	1630	287	346	146
FGF2	1717	2086	52	92	36
ERBB2	906	428	15	35	25
TGFB1	501	620	129	156	62
CYR61	262	126	1	4	3
MAP2K1	124	38	7	26	16
HRAS	83	51	2	5	1
CSF1	45	10	3	4	3
PDGFBB	33	6	3	3	0
EDN1	27	6	16	8	1
EDN3	24	0	0	1	0

Numbers indicate the number of publications listed on PubMed as of June 26th, 2019.

Table S8. Evaluation of published independent transcriptomic datasets. Comparison of differentially expressed genes from the discovery and adult asthma datasets.

Refer to MS Excel spreadsheet (supplementary).

Table S9. Evaluation of published independent transcriptomic datasets. Comparison of Reactome pathways from the discovery and adult asthma datasets.

Refer to MS Excel spreadsheet (supplementary).

Table S10. Evaluation of published independent transcriptomic datasets. Gene coexpression modules generated and association with recurrence of wheeze from the pediatric acute wheeze dataset.

Refer to MS Excel spreadsheet (supplementary).

Table S11. Evaluation of published independent transcriptomic datasets. Comparison of Reactome pathways from the discovery and pediatric acute wheeze datasets.

Refer to MS Excel spreadsheet (supplementary).

Table S12. Complete study participant demographics

	Non-wheeze	Wheeze	p value
No. children	110	91	N/A
Sex, M/F	67/43	59/32	0.661
Age at sampling, years [#]	5.9 (3.9-9.2)	4.9 (3.1-8.1)	0.057
Asthma Dx	0	37	***0.001 ****

No. – number; M – male; F, female; Dx – diagnosis; N/A – not applicable. [#]median (interquartile range); * $p<0.050$.

Table S13. Details of reference and target genes. List of all TaqMan primer/probe sets used in a TaqMan-based qPCR. *Reference gene.

Gene symbol	Gene name(s)	Taqman Assay ID	Amplicon length (bp)
*PPIA**	Peptidylprolyl isomerase A (cyclophilin A)	Hs99999904_m1	98
ITGAV	Integrin, alpha V	Hs00233808_m1	64
ITGA3	Integrin, alpha 3	Hs00233722_m1	69
ITGA5	Integrin, alpha 5	Hs01547673_m1	54
ITGB1	Integrin, beta 1	Hs00559595_m1	75
ITGB3	Integrin, beta 3	Hs01001469_m1	59
ITGB6	Integrin, beta 6	Hs00168458_m1	101

Movie S1. Overlaid cell migration trajectories during pAEC wound repair from children without wheeze.

Refer to video file (supplementary).

Movie S2. Overlaid cell migration trajectories during pAEC wound repair from children with wheeze.

Refer to video file (supplementary).

Supplemental Acknowledgements

The members of the Western Australian Epithelial Research Program (WAERP) are: Anthony Kicic, Stephen M. Stick, Darryl A. Knight, Elizabeth Kicic-Starcevich, Luke W. Garratt, Marc Padros-Goosen, Ee-Lyn Tan, Erika N. Sutanto, Kevin Looi, Jessica Hillas, Thomas Iosifidis, Nicole C. Shaw, Samuel T. Montgomery, Kak-Ming Ling, Kelly M. Martinovich, Francis J. Lannigan, Ricardo Bergesio, Bernard Lee, Shyan Vijayasekaran, Paul Swan, Mairead Heaney, Ian Forsyth, Tobias Schoep, Alexander Larcombe, Monica Hunter, Kate McGee, Nyssa Millington. The Australian Respiratory Epithelium Consortium (AusREC) acknowledges the following members: Anthony Kicic, Stephen M. Stick, Elizabeth Kicic-Starcevich, Luke W. Garratt, Erika N. Sutanto, Kevin Looi, Jessica Hillas, Thomas Iosifidis, Nicole C. Shaw, Samuel T. Montgomery, Kak-Ming Ling, Kelly M. Martinovich, Matthew W-P Poh, Daniel R. Laucirica, Craig Schofield, Samantha McLean, Katherine Landwehr, Nigel Farrow, Eugene Roscioli, David W. Parsons, Darryl A. Knight, Christopher Grainge, Andrew T. Reid, Su-Kim Loo, Punnam C. Veerati.